
MuDreamer: Learning Predictive World Models without Reconstruction

Maxime Burchi* Radu Timofte

Computer Vision Lab, CAIDAS & IFI, University of Würzburg, Germany

Abstract

The DreamerV3 agent recently demonstrated state-of-the-art performance in diverse domains, learning powerful world models in latent space using a pixel reconstruction loss. However, while the reconstruction loss is essential to Dreamer’s performance, it also necessitates modeling unnecessary information. Consequently, Dreamer sometimes fails to perceive crucial elements which are necessary for task-solving when visual distractions are present in the observation, significantly limiting its potential. In this paper, we present MuDreamer, a robust reinforcement learning agent that builds upon the DreamerV3 algorithm by learning a predictive world model without the need for reconstructing input signals. Rather than relying on pixel reconstruction, hidden representations are instead learned by predicting the environment value function and previously selected actions. Similar to predictive self-supervised methods for images, we find that the use of batch normalization is crucial to prevent learning collapse. We also study the effect of KL balancing between model posterior and prior losses on convergence speed and learning stability. We evaluate MuDreamer on the commonly used DeepMind Visual Control Suite and demonstrate stronger robustness to visual distractions compared to DreamerV3 and other reconstruction-free approaches, replacing the environment background with task-irrelevant real-world videos. Our method also achieves comparable performance on the Atari100k benchmark while benefiting from faster training.

1 Introduction

Deep reinforcement learning has achieved great success in recent years, solving complex tasks in diverse domains. Researchers made significant progress applying advances in deep learning for learning feature representations [41]. The use of deep neural networks as function approximations made it possible to train powerful agents directly from high-dimensional observations like images, achieving human to superhuman performance in challenging and visually complex domains like Atari games [42, 29], visual control [38, 6], the game of Go [53, 49], StarCraft II [58] and even Minecraft [4, 25]. However, these approaches generally require a large amount of environment interactions [56] or behavior cloning pretraining [51] to achieve strong performance.

To address this issue, concurrent works have chosen to focus on model-based approaches [52, 61], aiming to enhance the agent performance while reducing the number of necessary interactions with the environment. Reinforcement learning algorithms are typically categorized into two main groups: model-free algorithms, which directly learn value and/or policy functions through interaction with the environment, and model-based algorithms, which learn a model of the world. World models [55, 20] summarize an agent’s experience into a predictive model that can be used in place of the real environment to learn complex behaviors. This enables the agent to simulate multiple plausible trajectories in parallel, which not only enhances generalization but also improves sample efficiency.

*maxime.burchi@uni-wuerzburg.de

Recent works have shown that model-based agents can effectively be trained from images, leading to enhanced performance and sample efficiency compared to model-free approaches [22, 23, 33, 49, 24, 66, 40]. The DreamerV3 agent [25] recently demonstrated state-of-the-art performance across diverse domains, learning powerful world models in latent space using a pixel reconstruction loss. The agent solves long-horizon tasks from image inputs with both continuous and discrete action spaces. However, while the reconstruction loss is essential for Dreamer’s performance, it also necessitates modeling unnecessary information [44, 39, 43, 47, 15, 8]. Consequently, Dreamer sometimes fails to perceive crucial elements which are necessary for task-solving, significantly limiting its potential.

In this paper, we present MuDreamer, a robust reinforcement learning agent that builds upon the DreamerV3 [25] algorithm by learning a predictive world model without the necessity of reconstructing input signals. Taking inspiration from the MuZero [49] agent, MuDreamer learns a world model in latent space by predicting the environment rewards, continuation flags and value function, focusing on information relevant to the task. We also propose to incorporate an action prediction branch to predict the sequence of selected actions from the observed data. This additional task trains the world model to associate actions with environment changes and proves particularly beneficial for learning hidden representations in scenarios where environment rewards are extremely sparse. Similar to predictive self-supervised methods used for image data, we find that the use of batch normalization is crucial to prevent learning collapse in which the model produces constant or non-informative hidden states. Following Paster et al. [47], we solve this issue by introducing batch normalization inside the model representation network. We also study the effect of KL balancing between model posterior and prior losses on convergence speed and learning stability. We evaluate MuDreamer on the commonly used DeepMind Visual Control Suite [56] and demonstrate stronger robustness to visual distractions compared to DreamerV3 and other reconstruction-free approaches [43, 15]. MuDreamer learns to distinguish relevant details from unnecessary information when replacing the environment background with task-irrelevant real-world videos while DreamerV3 focuses on background details irrelevant to the task. Our method also achieves comparable performance on the Atari100k benchmark while benefiting from faster training.

2 Related Works

2.1 Model-based Reinforcement Learning

In recent years, there has been a growing interest in using neural networks as world models to simulate environments and train reinforcement learning agents from hypothetical trajectories. Initial research primarily focused on proprioceptive tasks [18, 52, 28, 60, 59], involving simple, low-dimensional environments. However, more recent efforts have shifted towards learning world models for environments with high-dimensional observations like images [33, 22, 23, 49, 66, 40]. For example, SimPLe [33] successfully demonstrated planning in Atari games by training a world model in pixel space and utilizing it to train a Proximal Policy Optimization (PPO) agent [50]. This approach involves a convolutional autoencoder for generating discrete latent variables and an LSTM-based recurrent network predicting latent bits autoregressively. PlaNet [22] proposed to learn a Recurrent State-Space Model (RSSM) in latent space using a pixel reconstruction loss, planning using model predictive control. Dreamer [23, 24, 25] extended PlaNet by incorporating actor and critic networks trained from simulated trajectories and imaginary rewards. MuZero [49] took a different approach, focusing on learning a model of the environment by predicting quantities crucial for planning, such as reward, action-selection policy, and value function. This approach allowed MuZero to excel in reinforcement learning tasks without relying on the reconstruction of input observations. EfficientZero [66] improved upon MuZero’s sample efficiency by incorporating a representation learning objective [12] to achieve better performance with limited data. Lastly, IRIS [40] proposed a discrete autoencoder [57] model for imagining trajectories, predicting discrete latent tokens in an autoregressive manner, using a transformer model.

2.2 Self-Supervised Representation Learning for Images

Self-Supervised Learning (SSL) of image representations has attracted significant research attention in recent years for its ability to learn hidden representations from large scale unlabelled datasets. Reconstruction-based approaches proposed to learn hidden representations by reconstructing a corrupted version of the input image [27, 64, 17]. Many works focused on pixel space reconstruction

while other proposed to predict hand-designed features like Histograms of Oriented Gradients (HOG) [62]. Contrastive approaches proposed to learn hidden representations using joint embedding architectures where output features of a sample and its distorted version are brought close to each other, while negative samples and their distortions are pushed away [31, 46, 26, 11]. These methods are commonly applied to Siamese architectures, where two identical networks are trained together, sharing parameters. In contrast, SwAV [9] proposed a different approach by ensuring consistency between cluster assignments produced for different augmentations of the same image, rather than directly comparing features. Predictive approaches proposed to predict the hidden representation of a similar view of the input signal without relying on negative samples [19, 10, 16, 12, 67, 3, 1]. These methods prevent learning collapse using various architectural tricks such as knowledge distillation [30], normalizing output representations, or the application of additional constraints to output representations like VICReg [5].

2.3 Reconstruction-Free Dreamer

Following advances in the area of self-supervised representation learning for image data, several works proposed to apply reconstruction-free representation learning techniques to Dreamer. The original Dreamer paper [23] initially experimented with contrastive learning [46] to learn representations having maximal mutual information with the encoded observation but found that it did not match the performance of reconstruction-based representations. Subsequently, several works proposed Dreamer variants using contrastive learning [44, 39, 43, 45, 8], successfully competing with Dreamer on several tasks of the Visual Control Suite. Dreaming [44] proposed to use a multi-step InfoNCE loss to sequentially predict future time steps representations of augmented views. Temporal Predictive Coding (TPC) [43] followed a similar approach using contrastive learning to maximize the mutual information between past and the future latent states. DreamerPro [15] proposed to encourage uniform cluster assignment across batches of samples, implicitly pushing apart embeddings of different observations. Concurrently, BLAST [47] proposed to learn hidden representation using a slow-moving teacher network to generate target embeddings [19]. BLAST also demonstrated that batch normalization was critical to the agent performance. In this paper, we present a reconstruction-free variant of DreamerV3 achieving comparable performance without using negatives samples, separate augmented views of images, or an additional slow-moving teacher encoder network.

3 Background

3.1 Dreamer

Our method is built on the DreamerV3 [25] algorithm which we refer to as Dreamer throughout the paper. Dreamer [23] is an actor-critic model-based reinforcement learning algorithm learning a powerful predictive world model from past experience in latent space using a replay buffer. The world model is learned from self-supervised learning by predicting the environment reward, episode continuation and next latent state given previously selected actions. The algorithm also uses a pixel reconstruction loss using an autoencoder architecture such that all information about the observations must pass through the model hidden state. The actor and critic neural networks learn behaviors purely from abstract sequences predicted by the world model. The model generates simulated trajectories from replayed experience states using the actor network to sample actions. The value network is trained to predict the sum of future reward while the actor network is trained to maximize the expected sum of future reward from the value network.

DreamerV2 [24] applied Dreamer to Atari games, utilizing categorical latent states with straight-through gradients [7] in the world model to improve performance, instead of Gaussian latents with reparameterized gradients [35]. It also introduced KL balancing, separately scaling the prior cross entropy and the posterior entropy in the KL loss to encourage learning an accurate temporal prior.

DreamerV3 [25] mastered diverse domains using the same hyper-parameters with a set of architectural changes to stabilize learning across tasks. The agent uses Symlog predictions for the reward and value function to address the scale variance across domains. The networks also employ layer normalization [2] to improve robustness and performance while scaling up to larger model sizes. It regularizes the policy by normalizing the returns and value function using an Exponential Moving Average (EMA) of the returns percentiles. Using these modifications, the agent solves Atari games and DeepMind Control tasks while collecting diamonds in Minecraft.

3.2 MuZero

MuZero [49] is a model-based algorithm combining Monte-Carlo Tree Search (MCTS) [14] with a world model to achieve superhuman performance in precision planning tasks such as Chess, Shogi and Go. The model is learned by being unrolled recurrently for K steps and predicting environment quantities relevant to planning. All parameters of the model are trained jointly to accurately match the TD value [54] and reward, for every hypothetical step k . The MCTS algorithm uses the learned model to simulate environment trajectories and output an action visit distribution over the root node. This potentially better policy compared to the neural network one is used to train the policy network. MuZero excels in discrete action domains but struggles with high-dimensional continuous action spaces, where a discretization of possible actions is required to apply MCTS [66]. Our proposed method, MuDreamer, draws inspiration from MuZero to learn a world model by predicting the expected sum of future rewards. MuDreamer solves tasks from pixels in both continuous and discrete action space, without the need for a reconstruction loss.

4 MuDreamer

We present MuDreamer, a reconstruction-free variant of the Dreamer algorithm, which learns a world model in latent space by predicting not only rewards and continuation flags but also the environment value function and previously selected actions. Figure 1 illustrates the learning process of the MuDreamer world model. Similar to Dreamer, MuDreamer comprises three neural networks: a world model, a critic network, and an actor network. These three networks are trained concurrently using an experience replay buffer that collects past experiences. This section provides an overview of the world model and the modifications applied to the Dreamer agent. We also detail the learning process of the critic and actor networks.

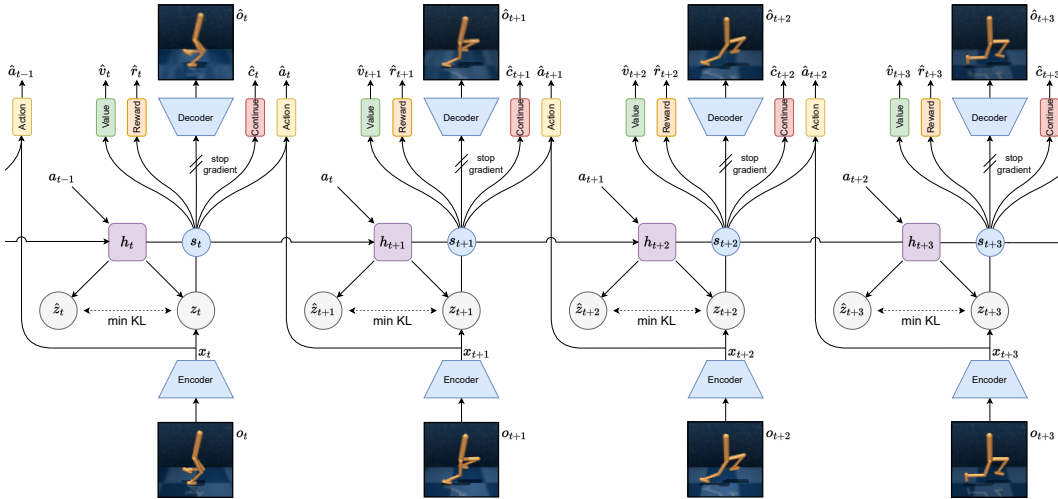


Figure 1: MuDreamer world model training. A sequence of image observations $o_{1:T}$ is sampled from the replay buffer. The sequence is mapped to hidden representations $x_{1:T}$ using a CNN encoder. At each step, the RSSM computes a posterior state z_t representing the current observation o_t and a prior state \hat{z}_t that predict the posterior without having access to the current observation. Unlike Dreamer, the decoder gradients are not back-propagated to the rest of the model. The hidden representations are learned solely using value, reward, episode continuation and action prediction heads.

4.1 World Model Learning

Following DreamerV3, we learn a world model in latent space, using a Convolutional Neural Network (CNN) [37] encoder to map high-dimensional visual observations o_t to hidden representations x_t . The world model is implemented as a Recurrent State-Space Model (RSSM) [22] composed of three sub networks: A sequential network using a Gated Recurrent Unit (GRU) [13] to predict the next hidden state h_t given past action a_{t-1} . A representation network predicting the current stochastic

state z_t using both h_t and encoded features x_t . And a dynamics network predicting the stochastic state z_t given the current recurrent state h_t . The concatenation of h_t and z_t forms the model hidden state $s_t = \{h_t, z_t\}$ from which we predict environment rewards r_t , episode continuation $c_t \in \{0, 1\}$ and value function v_t . We also learn an action predictor network using encoded features x_t and preceding model hidden state s_{t-1} to predict the action which led to the observed environment change. The trainable world model components are the following:

$$\text{RSSM} \left\{ \begin{array}{ll} \text{Encoder:} & x_t = \text{enc}_\phi(o_t) \\ \text{Sequential Network:} & h_t = f_\phi(h_{t-1}, z_{t-1}, a_{t-1}) \\ \text{Representation Network:} & z_t \sim q_\phi(z_t | h_t, x_t) \\ \text{Dynamics Predictor:} & \hat{z}_t \sim p_\phi(\hat{z}_t | h_t) \\ \text{Reward Predictor:} & \hat{r}_t \sim p_\phi(\hat{r}_t | s_t) \\ \text{Continue Predictor:} & \hat{c}_t \sim p_\phi(\hat{c}_t | s_t) \\ \text{Value Predictor:} & \hat{v}_t \sim p_\phi(\hat{v}_t | s_t) \\ \text{Action Predictor:} & \hat{a}_{t-1} \sim p_\phi(\hat{a}_{t-1} | x_t, s_{t-1}) \\ \text{Decoder (auxiliary):} & \hat{o}_t \sim p_\phi(\hat{o}_t | \text{sg}(s_t)) \end{array} \right. \quad (1)$$

Given a sequence batch of inputs $x_{1:T}$, actions $a_{1:T}$, rewards $r_{1:T}$, and continuation flags $c_{1:T}$, the world model parameters (ϕ) are optimized end-to-end to minimize a prediction loss L_{pred} , dynamics loss L_{dyn} , and representation loss L_{rep} with corresponding loss weights $\beta_{pred} = 1.0$, $\beta_{dyn} = 0.95$ and $\beta_{rep} = 0.05$. The loss function for learning the world model is:

$$L_{model}(\phi) = \mathbb{E}_{q_\phi} \left[\sum_{t=1}^T (\beta_{pred} L_{pred}(\phi) + \beta_{dyn} L_{dyn}(\phi) + \beta_{rep} L_{rep}(\phi)) \right] \quad (2)$$

The prediction loss trains the reward, continue, value and action predictors to learn hidden representations. We optionally learn an auxiliary decoder network to reconstruct the sequence of observations using the stop gradient operator $\text{sg}(\cdot)$ to prevent the gradients from being back-propagated to other network parameters. The auxiliary decoder reconstruction loss has no effect on MuDreamer training and the decoder is excluded from total number of parameters. The dynamics loss trains the dynamics predictor to predict the next representation by minimizing the KL divergence between the predictor $p_\phi(\hat{z}_t | h_t)$ and the next stochastic representation $q_\phi(z_t | h_t, x_t)$. While the representation loss trains the representations to become more predictable if the dynamics cannot predict their distribution:

$$\begin{aligned} L_{pred}(\phi) = & \underbrace{-\log p_\phi(r_t | s_t)}_{\text{reward predictor loss}} + \underbrace{-\log p_\phi(c_t | s_t)}_{\text{continue predictor loss}} + \underbrace{-\log p_\phi(R_t^\lambda | s_t)}_{\text{value predictor loss}} \\ & + \underbrace{-\log p_\phi(a_{t-1} | x_t, s_{t-1})}_{\text{action predictor loss}} + \underbrace{-\log p_\phi(o_t | \text{sg}(s_t))}_{\text{reconstruction loss (auxiliary)}} \end{aligned} \quad (3)$$

$$\begin{aligned} L_{dyn}(\phi) &= \max(1, \text{KL}[\text{sg}(q_\phi(z_t | h_t, x_t)) \parallel p_\phi(\hat{z}_t | h_t)]) \\ L_{rep}(\phi) &= \max(1, \text{KL}[q_\phi(z_t | h_t, x_t) \parallel \text{sg}(p_\phi(\hat{z}_t | h_t))]) \end{aligned} \quad (4)$$

Value Predictor We use a value network to predict the environment value function from the model hidden state. The value function aims to represent the expected λ -returns [54] with λ set 0.95, using a slow moving target value predictor $v_{\phi'}$ with EMA momentum $\tau = 0.01$:

$$R_t^\lambda = r_{t+1} + \gamma c_{t+1} \left((1 - \lambda) v_{\phi'}(s_{t+1}) + \lambda R_{t+1}^\lambda \right) \quad R_T^\lambda = v_{\phi'}(s_T) \quad (5)$$

Following previous works [49, 25], we set the discount factor γ to 0.997 and use a discrete regression of λ -returns to let the critic maintain and refine a distribution over potential returns. The λ -return targets are first transformed using the Symlog function and discretized using a *twohot* encoding. Given twohot-encoded target returns $y_t = \text{sg}(\text{twohot}(\text{symlog}(R_t^\lambda)))$ the value predictor minimizes the categorical cross entropy loss with the predicted value logits.

Action Predictor The action predictor network learns to identify the previously selected actions for each time step of the sampled trajectory. It shares the same architecture as the actor network but takes the current encoded features x_t and preceding model hidden state s_{t-1} as inputs. Since the current model hidden state s_t already depends of the action target a_t .

Batch Normalization In order to prevent learning collapse to constant or non-informative model states, like observed in predictive self-supervised learning for image data [19, 11], we apply batch normalization [32] to MuDreamer. Following BLAST [47], we replace the hidden normalization layer inside the representation network by a batch normalization layer. We find that it is sufficient to prevent collapse on all tasks and stabilize learning.

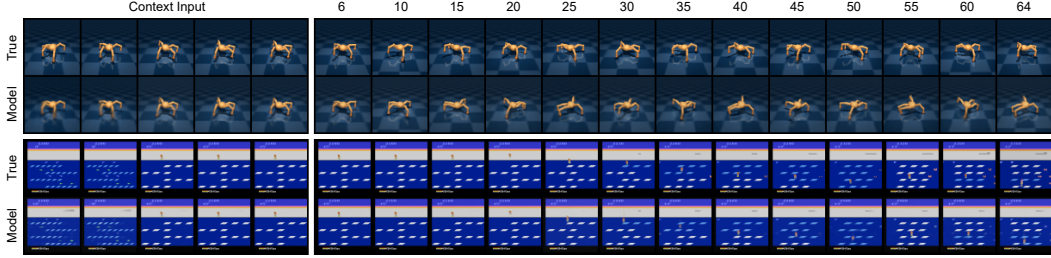


Figure 2: Reconstruction of MuDreamer model predictions over 64 time steps. We take 5 context frames and generate trajectories of 59 steps into the future using the model sequential and dynamics networks. Actions are predicted using the policy network given generated latent states. MuDreamer generates accurate long-term predictions similar to Dreamer without requiring reconstruction loss gradients during training to compress the observation information into the model hidden state.

4.2 Behavior Learning

Following DreamerV3 [25], MuDreamer policy and value functions are learned by imagining trajectories using the world model (Figure 2). Actor-critic learning takes place entirely in latent space, allowing the agent to use a large batch size of imagined trajectories. To do so, the model hidden states of the sampled sequence are flattened along batch and time dimensions. The world model imagines $H = 15$ steps into the future using the sequential and dynamics networks, selecting actions from the actor. The actor and critic use parameter vectors (θ) and (ψ), respectively:

$$\text{Actor: } a_t \sim \pi_\theta(a_t | \hat{s}_t) \quad \text{Critic: } v_\psi(\hat{s}_t) \approx \mathbb{E}_{p_\psi \pi_\theta}[\hat{R}_t^\lambda] \quad (6)$$

Critic Learning Similarly to the value predictor branch, the critic is trained by predicting the discretized λ -returns, but using rewards predictions imagined by the world model:

$$\hat{R}_t^\lambda = \hat{r}_{t+1} + \gamma \hat{c}_{t+1} \left((1 - \lambda) v_\psi(\hat{s}_{t+1}) + \lambda \hat{R}_{t+1}^\lambda \right) \quad \hat{R}_{H+1}^\lambda = v_\psi(\hat{s}_{H+1}) \quad (7)$$

The critic also does not use a target network but relies on its own predictions for estimating rewards beyond the prediction horizon. This requires stabilizing the critic by adding a regularizing term of the predicted values toward the outputs of its own EMA network:

$$L_{\text{critic}}(\psi) = \sum_{t=1}^H \left(\underbrace{-\log p_\psi(\hat{R}_t^\lambda | \hat{s}_t)}_{\text{discrete returns regression}} - \underbrace{\log p_\psi(v_\psi(\hat{s}_t) | \hat{s}_t)}_{\text{critic EMA regularizer}} \right) \quad (8)$$

Actor Learning The actor network learns to select actions that maximize advantages $A_t^\lambda = (\hat{R}_t^\lambda - v_\psi(\hat{s}_t)) / \max(1, S)$ while regularizing the policy entropy to ensure exploration both in imagination and during data collection. In order to use a single regularization scale for all domains, DreamerV3 stabilizes the scale of returns using exponentially moving average statistics of their percentiles: $S = \text{EMA}(\text{Per}(\hat{R}_t^\lambda, 95) - \text{Per}(\hat{R}_t^\lambda, 5), 0.99)$. The actor loss computes policy gradients using stochastic back-propagation through the model sequential and dynamics networks for continuous actions ($\rho = 0$) and using reinforce [63] for discrete actions ($\rho = 1$):

$$L_{\text{actor}}(\theta) = \sum_{t=1}^H \left(\underbrace{-\rho \log \pi_\theta(a_t | \hat{s}_t) \text{sg}(A_t^\lambda)}_{\text{reinforce}} - \underbrace{(1 - \rho) A_t^\lambda}_{\text{dynamics backprop}} - \underbrace{\eta \text{H}[\pi_\theta(a_t | \hat{s}_t)]}_{\text{entropy regularizer}} \right) \quad (9)$$

5 Experiments

In this section, we aim to evaluate the performance of our MuDreamer algorithm compared to its reconstruction-based version and other published model-based and model-free methods. We evaluate MuDreamer on the Visual Control Suite from DeepMind (Table 1) and under the natural background setting (Table 2) where tasks background is replaced by real-world videos. We also proceed to a detailed ablation study, studying the effect of batch normalization, action-value predictors and KL balancing on performance and learning stability (Table 3). The performance curves showing comparison for each individual task, Atari100k benchmark comparison with other model-based methods, as well as additional visualizations can be found in the appendix.

5.1 Visual Control Suite

The DeepMind Control Suite was introduced by Tassa et al. [56] as a set of continuous control tasks with a standardised structure and interpretable rewards. The suite is intended to serve as performance benchmarks for reinforcement learning agents in continuous action space. The tasks can be solved from low-dimensional inputs and/or pixel observations. In this work, we evaluate our method on the Visual Control Suite benchmark which contains 20 tasks where the agent receives only high-dimensional images as inputs and a budget of 1M environment steps. Similarly to DreamerV3 [25], we use 4 environment instances during training with a training ratio of 512 replayed steps per policy step. Our PyTorch [48] implementation of MuDreamer takes a little less than 14 hours to reach 1M environment steps on the *Walker Run* visual control task using a single NVIDIA RTX 3090 GPU and 16 CPU cores, while DreamerV3 takes 15 hours. The total amount of trainable parameters for MuDreamer and DreamerV3 are 15.3M and 17.9M, respectively.

Table 1: Visual Control Suite scores (1M environment steps). † results were taken from Hafner et al. [25]. We average the evaluation score over 10 episodes and use 3 different seeds per experiment.

Task	SAC†	CURL†	DrQ-v2†	DreamerV3†	MuDreamer
Acrobot Swingup	5.1	5.1	128.4	210.0	304.6
Cartpole Balance	963.1	979.0	991.5	996.4	990.4
Cartpole Balance Sparse	950.8	981.0	996.2	1000.0	1000.0
Cartpole Swingup	692.1	762.7	858.9	819.1	823.0
Cartpole Swingup Sparse	154.6	236.2	706.9	792.9	582.0
Cheetah Run	27.2	474.3	691.0	728.7	872.5
Cup Catch	163.9	965.5	931.8	957.1	930.8
Finger Spin	312.2	877.1	846.7	818.5	603.6
Finger Turn Easy	176.7	338.0	448.4	787.7	915.4
Finger Turn Hard	70.5	215.6	220.0	810.8	886.5
Hopper Hop	3.1	152.5	189.9	369.6	311.8
Hopper Stand	5.2	786.8	893.0	900.6	883.9
Pendulum Swingup	560.1	376.4	839.7	806.3	806.7
Quadruped Run	50.5	141.5	407.0	352.3	627.8
Quadruped Walk	49.7	123.7	660.3	352.6	860.0
Reacher Easy	86.5	609.3	910.2	898.9	907.0
Reacher Hard	9.1	400.2	572.9	499.2	733.0
Walker Run	26.9	376.2	517.1	757.8	740.9
Walker Stand	159.3	463.5	974.1	976.7	964.3
Walker Walk	38.9	828.8	762.9	955.8	949.8
Mean	225.3	504.7	677.4	739.6	784.7
Median	78.5	431.8	734.9	808.5	849.6

Table 1 compares MuDreamer with DreamerV3 and other recent methods on the Visual Control Suite using 1M environment steps. MuDreamer achieves state-of-the-art mean-score without reconstructing the input signal, outperforming SAC [21], CURL [36], DrQ-v2 [65] and DreamerV3. As shown in Figure 2, although the reconstruction gradients are not propagated to the whole network, the decoder easily reconstruct the input image, meaning that the model hidden state contains all necessary information about the environment. We find that MuDreamer achieves better performance and learning stability on tasks like *Finger Turn Hard* and *Reacher Hard* where crucial task-solving elements are small and harder to model using reconstruction.

5.2 Natural Background Setting

While the reconstruction loss is essential for Dreamer’s performance, it also necessitates modeling unnecessary information. Consequently, Dreamer sometimes fails to perceive crucial elements which are necessary for task-solving when visual distractions are present in the observation, significantly limiting its potential. This object vanishing phenomenon arises particularly when crucial elements are small like the ball in *Cup Catch*. In order to further study the effect of visual distractions on DreamerV3 and MuDreamer performance, we experiment with the natural background setting [39, 43, 15, 8], where the DeepMind Visual Control tasks background is replaced by real-world videos. Following TPC [43] and DreamerPro [15], we replace the background by task-irrelevant videos randomly sampled from the *driving car* class of the Kinetics 400 dataset [34]. We also use two separate sets of background videos for training and evaluation in order to test generalization to unseen distractions. Table 2 shows the comparison of MuDreamer with DreamerV3, DreamerPro and TPC on the Visual Control Suite under the natural background setting. MuDreamer successfully

learns a policy on most tasks and achieves state-of-the-art performance with a mean-score of 517.0 compared to 445.2 and 372.8 for DreamerPro and TPC. Figure 3 shows the decoder reconstruction of observations by DreamerV3 and MuDreamer on *Walker Run*, *Finger Spin* and *Quadruped Run* tasks. MuDreamer correctly reconstructs the agent body with a monochrome or blurry background while DreamerV3 focuses on the background details, discarding the agent body and necessary information.

Table 2: Visual Control Suite scores under the natural background setting (1M env. steps). † denotes our tested reimplementaion of DreamerV3. ‡ results were obtained using the official implementation of DreamerPro. We average the evaluation score over 10 episodes and use 3 seeds per experiment.

Task	Random	TPC [‡]	DreamerPro [‡]	DreamerV3 [†]	MuDreamer
Acrobot Swingup	0.3	5.1	13.1	9.1	41.9
Cartpole Balance	329.3	792.9	870.1	198.7	974.8
Cartpole Balance Sparse	53.9	26.9	198.4	18.4	898.7
Cartpole Swingup	67.4	574.8	689.2	145.7	794.4
Cartpole Swingup Sparse	0.0	0.2	17.8	0.3	0.0
Cheetah Run	6.7	440.8	380.7	94.3	318.1
Cup Catch	31.5	451.5	437.5	27.9	904.5
Finger Spin	0.9	696.8	724.2	96.5	644.2
Finger Turn Easy	48.8	479.5	232.4	197.8	229.4
Finger Turn Hard	35.0	198.3	228.3	39.8	226.7
Hopper Hop	0.0	0.2	1.4	0.6	0.2
Hopper Stand	1.9	14.5	296.5	3.0	5.4
Pendulum Swingup	2.0	778.7	777.6	8.0	606.8
Quadruped Run	8.8	162.9	470.8	108.9	735.0
Quadruped Walk	110.0	681.4	784.5	61.2	872.8
Reacher Easy	52.6	642.4	692.7	154.2	914.4
Reacher Hard	7.4	7.0	9.4	10.6	13.5
Walker Run	25.9	137.9	402.9	78.7	432.8
Walker Stand	139.4	935.4	940.6	254.4	966.7
Walker Walk	36.8	428.3	736.1	164.7	759.0
Mean	47.9	372.8	445.2	83.6	517.0
Median	28.7	409.8	416.2	57.1	620.0

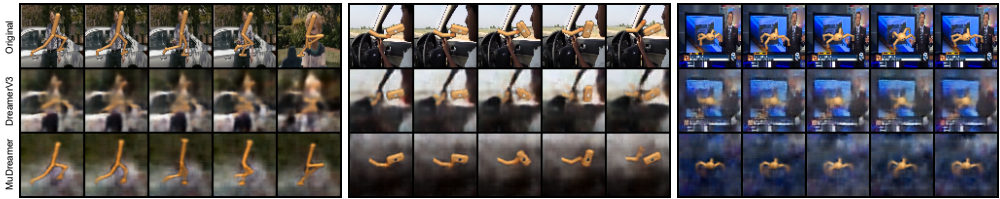


Figure 3: Agents reconstruction of observations using natural backgrounds for *Walker Run*, *Finger Spin* and *Quadruped Run* tasks. First row shows original sequence of observation, second row shows DreamerV3 reconstruction and third row MuDreamer decoder reconstruction. We observe that DreamerV3 reconstructs general details while MuDreamer learns to filter unnecessary information.

5.3 Ablation Study

In order to understand the necessary components of MuDreamer, we conduct ablation studies applying one modification at a time. We study the impact of using value and action prediction branches, removing one or both branches during training. We study the effect of using batch normalization in the representation network to stabilize learning and avoid collapse without the reconstruction loss. We also study the effect of KL balancing hyper-parameters on learning speed and stability. We perform all these ablation studies on the Visual Control Suite, observing the effect of each modification for diverse tasks. The mean and median score results of these studies are summarized in Table 3 and Figure 4. Please refer to the appendix for the evaluation curves of individual tasks.

Action-Value Predictors We study the necessity of using action and value prediction branches to learn hidden representations and successfully solve the tasks without reconstruction loss. We observed that removing the action or value prediction heads led to a degradation of MuDreamer performance and decoder reconstruction quality on most of the Visual Control tasks. The action and value prediction losses require the model to learn environment dynamics which leads to more accurate model predictions and better performance.

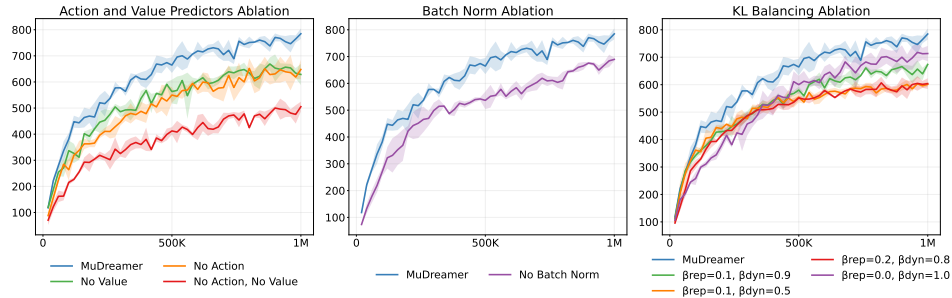


Figure 4: Ablations mean scores on the Visual Control Suite using 1M environment steps.

Table 3: Ablations evaluated on 20 tasks of the Visual Control Suite using 1M environment steps. Each ablation applies only one modification to the MuDreamer agent.

Agent	Mean	Median	Task Score \geq MuDreamer
MuDreamer	784.7	849.6	
No Value Predictor	628.8	745.6	5 / 20
No Action Predictor	648.0	810.8	6 / 20
No Action and Value Predictors	505.4	493.2	4 / 20
No Batch Normalization	689.5	820.7	8 / 20
$\beta_{rep} = 0.0, \beta_{dyn} = 1.0$	713.5	824.3	6 / 20
$\beta_{rep} = 0.1, \beta_{dyn} = 0.9$	673.7	845.7	8 / 20
$\beta_{rep} = 0.1, \beta_{dyn} = 0.5$	601.1	790.2	10 / 20
$\beta_{rep} = 0.2, \beta_{dyn} = 0.8$	603.9	694.5	5 / 20

Batch Normalization We study the effect of using batch normalization instead of layer normalization inside the representation network to stabilize representation learning. We find that batch normalization prevents collapse in which the model produces constant or non-informative hidden states. Without batch normalization, we observe that MuDreamer fails to learn representations for some of the tasks. The standard deviation of the model encoded features x_t converges to zero, which prevent learning hidden representations. Batch normalization solves this problem by stabilizing dynamics and representation losses.

KL Balancing We find that applying the default KL balancing parameters of DreamerV3 ($\beta_{dyn} = 0.5, \beta_{rep} = 0.1$) slows down convergence for some of the tasks, restraining the model from learning representations. A larger regularization of the posterior toward the prior with $\beta_{rep} = 0.2$ limits the amount of information encoded in the model stochastic state. We observe that unnecessary information such as the environment floor and the agent shadow are sometimes reconstructed as monochrome surfaces without the original details. Similar to BLAST and predictive SSL approaches [19, 11], we experiment using the stop gradient operation with $\beta_{rep} = 0.0$. We find that this solves the issue but generates learning instabilities with spikes for the dynamics and prediction losses. We suppose this create difficulties for the prior to predict posterior representations since we do not use a slow moving teacher encoder network. Using a slight regularization of the representations with $\beta_{rep} = 0.05$ solved both of these issues.

6 Conclusion

We presented MuDreamer, a robust reinforcement learning agent solving control tasks from image inputs with continuous and discrete action spaces, all without the need to reconstruct input signals. MuDreamer learns a world model by predicting environment rewards, value function, and continuation flags, focusing on information relevant to the task. We also proposed to incorporate an action prediction branch to predict the sequence of selected actions. MuDreamer demonstrates stronger robustness to visual distractions on the DeepMind Visual Control Suite compared to DreamerV3 and other methods when the environment background is replaced by task-irrelevant real-world videos. Our approach also benefits from faster training, as it does not require training an additional decoder network or encoding separate augmented views of the observation to learn hidden representations.

References

- [1] Mahmoud Assran, Quentin Duval, Ishan Misra, Piotr Bojanowski, Pascal Vincent, Michael Rabbat, Yann LeCun, and Nicolas Ballas. Self-supervised learning from images with a joint-embedding predictive architecture. In *Proceedings of the IEEE/CVF Conference on Computer Vision and Pattern Recognition*, pages 15619–15629, 2023.
- [2] Jimmy Lei Ba, Jamie Ryan Kiros, and Geoffrey E Hinton. Layer normalization. *arXiv preprint arXiv:1607.06450*, 2016.
- [3] Alexei Baevski, Wei-Ning Hsu, Qiantong Xu, Arun Babu, Jiatao Gu, and Michael Auli. Data2vec: A general framework for self-supervised learning in speech, vision and language. In *International Conference on Machine Learning*, pages 1298–1312. PMLR, 2022.
- [4] Bowen Baker, Ilge Akkaya, Peter Zhokov, Joost Huizinga, Jie Tang, Adrien Ecoffet, Brandon Houghton, Raul Sampedro, and Jeff Clune. Video pretraining (vpt): Learning to act by watching unlabeled online videos. *Advances in Neural Information Processing Systems*, 35:24639–24654, 2022.
- [5] Adrien Bardes, Jean Ponce, and Yann LeCun. Vicreg: Variance-invariance-covariance regularization for self-supervised learning. *arXiv preprint arXiv:2105.04906*, 2021.
- [6] Gabriel Barth-Maron, Matthew W. Hoffman, David Budden, Will Dabney, Dan Horgan, Dhruva TB, Alistair Muldal, Nicolas Heess, and Timothy Lillicrap. Distributional policy gradients. In *International Conference on Learning Representations*, 2018.
- [7] Yoshua Bengio, Nicholas Léonard, and Aaron Courville. Estimating or propagating gradients through stochastic neurons for conditional computation. *arXiv preprint arXiv:1308.3432*, 2013.
- [8] Homanga Bharadhwaj, Mohammad Babaeizadeh, Dumitru Erhan, and Sergey Levine. Information prioritization through empowerment in visual model-based rl. In *International Conference on Learning Representations*, 2022.
- [9] Mathilde Caron, Ishan Misra, Julien Mairal, Priya Goyal, Piotr Bojanowski, and Armand Joulin. Unsupervised learning of visual features by contrasting cluster assignments. *Advances in neural information processing systems*, 33:9912–9924, 2020.
- [10] Mathilde Caron, Hugo Touvron, Ishan Misra, Hervé Jégou, Julien Mairal, Piotr Bojanowski, and Armand Joulin. Emerging properties in self-supervised vision transformers. In *Proceedings of the IEEE/CVF international conference on computer vision*, pages 9650–9660, 2021.
- [11] Ting Chen, Simon Kornblith, Mohammad Norouzi, and Geoffrey Hinton. A simple framework for contrastive learning of visual representations. In *International conference on machine learning*, pages 1597–1607. PMLR, 2020.
- [12] Xinlei Chen and Kaiming He. Exploring simple siamese representation learning. In *Proceedings of the IEEE/CVF conference on computer vision and pattern recognition*, pages 15750–15758, 2021.
- [13] Kyunghyun Cho, Bart Van Merriënboer, Caglar Gulcehre, Dzmitry Bahdanau, Fethi Bougares, Holger Schwenk, and Yoshua Bengio. Learning phrase representations using rnn encoder-decoder for statistical machine translation. *arXiv preprint arXiv:1406.1078*, 2014.
- [14] Rémi Coulom. Efficient selectivity and backup operators in monte-carlo tree search. In *International conference on computers and games*, pages 72–83. Springer, 2006.
- [15] Fei Deng, Ingook Jang, and Sungjin Ahn. Dreamerpro: Reconstruction-free model-based reinforcement learning with prototypical representations. In *International Conference on Machine Learning*, pages 4956–4975. PMLR, 2022.
- [16] Aleksandr Ermolov, Aliaksandr Siarohin, Enver Sangineto, and Nicu Sebe. Whitening for self-supervised representation learning. In *International Conference on Machine Learning*, pages 3015–3024. PMLR, 2021.

- [17] Christoph Feichtenhofer, Yanghao Li, Kaiming He, et al. Masked autoencoders as spatiotemporal learners. *Advances in neural information processing systems*, 35:35946–35958, 2022.
- [18] Yarin Gal, Rowan McAllister, and Carl Edward Rasmussen. Improving pilco with bayesian neural network dynamics models. In *Data-efficient machine learning workshop, ICML*, volume 4, page 25, 2016.
- [19] Jean-Bastien Grill, Florian Strub, Florent Alché, Corentin Tallec, Pierre Richemond, Elena Buchatskaya, Carl Doersch, Bernardo Avila Pires, Zhaohan Guo, Mohammad Gheshlaghi Azar, et al. Bootstrap your own latent—a new approach to self-supervised learning. *Advances in neural information processing systems*, 33:21271–21284, 2020.
- [20] David Ha and Jürgen Schmidhuber. World models. *arXiv preprint arXiv:1803.10122*, 2018.
- [21] Tuomas Haarnoja, Aurick Zhou, Pieter Abbeel, and Sergey Levine. Soft actor-critic: Off-policy maximum entropy deep reinforcement learning with a stochastic actor. In *International conference on machine learning*, pages 1861–1870. PMLR, 2018.
- [22] Danijar Hafner, Timothy Lillicrap, Ian Fischer, Ruben Villegas, David Ha, Honglak Lee, and James Davidson. Learning latent dynamics for planning from pixels. In *International conference on machine learning*, pages 2555–2565. PMLR, 2019.
- [23] Danijar Hafner, Timothy Lillicrap, Jimmy Ba, and Mohammad Norouzi. Dream to control: Learning behaviors by latent imagination. In *International Conference on Learning Representations*, 2020.
- [24] Danijar Hafner, Timothy Lillicrap, Mohammad Norouzi, and Jimmy Ba. Mastering atari with discrete world models. In *International Conference on Learning Representations*, 2021.
- [25] Danijar Hafner, Jurgis Pasukonis, Jimmy Ba, and Timothy Lillicrap. Mastering diverse domains through world models. *arXiv preprint arXiv:2301.04104*, 2023.
- [26] Kaiming He, Haoqi Fan, Yuxin Wu, Saining Xie, and Ross Girshick. Momentum contrast for unsupervised visual representation learning. In *Proceedings of the IEEE/CVF conference on computer vision and pattern recognition*, pages 9729–9738, 2020.
- [27] Kaiming He, Xinlei Chen, Saining Xie, Yanghao Li, Piotr Dollár, and Ross Girshick. Masked autoencoders are scalable vision learners. In *Proceedings of the IEEE/CVF conference on computer vision and pattern recognition*, pages 16000–16009, 2022.
- [28] Mikael Henaff, William F Whitney, and Yann LeCun. Model-based planning with discrete and continuous actions. *arXiv preprint arXiv:1705.07177*, 2017.
- [29] Matteo Hessel, Joseph Modayil, Hado Van Hasselt, Tom Schaul, Georg Ostrovski, Will Dabney, Dan Horgan, Bilal Piot, Mohammad Azar, and David Silver. Rainbow: Combining improvements in deep reinforcement learning. In *Proceedings of the AAAI conference on artificial intelligence*, volume 32, 2018.
- [30] Geoffrey Hinton, Oriol Vinyals, and Jeff Dean. Distilling the knowledge in a neural network. *arXiv preprint arXiv:1503.02531*, 2015.
- [31] R Devon Hjelm, Alex Fedorov, Samuel Lavoie-Marchildon, Karan Grewal, Phil Bachman, Adam Trischler, and Yoshua Bengio. Learning deep representations by mutual information estimation and maximization. In *International Conference on Learning Representations*, 2019.
- [32] Sergey Ioffe and Christian Szegedy. Batch normalization: Accelerating deep network training by reducing internal covariate shift. In *International conference on machine learning*, pages 448–456. pmlr, 2015.
- [33] Lukasz Kaiser, Mohammad Babaeizadeh, Piotr Milos, Blazej Osinski, Roy H Campbell, Konrad Czechowski, Dumitru Erhan, Chelsea Finn, Piotr Kozakowski, Sergey Levine, et al. Model-based reinforcement learning for atari. In *International Conference on Learning Representations*, 2020.

- [34] Will Kay, Joao Carreira, Karen Simonyan, Brian Zhang, Chloe Hillier, Sudheendra Vijayanarasimhan, Fabio Viola, Tim Green, Trevor Back, Paul Natsev, et al. The kinetics human action video dataset. *arXiv preprint arXiv:1705.06950*, 2017.
- [35] Diederik P Kingma and Max Welling. Auto-encoding variational bayes. *arXiv preprint arXiv:1312.6114*, 2013.
- [36] Michael Laskin, Aravind Srinivas, and Pieter Abbeel. Curl: Contrastive unsupervised representations for reinforcement learning. In *International Conference on Machine Learning*, pages 5639–5650. PMLR, 2020.
- [37] Yann LeCun, Bernhard Boser, John S Denker, Donnie Henderson, Richard E Howard, Wayne Hubbard, and Lawrence D Jackel. Backpropagation applied to handwritten zip code recognition. *Neural computation*, 1(4):541–551, 1989.
- [38] Timothy P Lillicrap, Jonathan J Hunt, Alexander Pritzel, Nicolas Heess, Tom Erez, Yuval Tassa, David Silver, and Daan Wierstra. Continuous control with deep reinforcement learning. In *International Conference on Learning Representations*, 2016.
- [39] Xiao Ma, Siwei Chen, David Hsu, and Wee Sun Lee. Contrastive variational reinforcement learning for complex observations. In *Conference on Robot Learning*, pages 959–972. PMLR, 2021.
- [40] Vincent Micheli, Eloi Alonso, and François Fleuret. Transformers are sample efficient world models. In *International Conference on Learning Representations*, 2023.
- [41] Volodymyr Mnih, Koray Kavukcuoglu, David Silver, Alex Graves, Ioannis Antonoglou, Daan Wierstra, and Martin Riedmiller. Playing atari with deep reinforcement learning. *arXiv preprint arXiv:1312.5602*, 2013.
- [42] Volodymyr Mnih, Koray Kavukcuoglu, David Silver, Andrei A Rusu, Joel Veness, Marc G Bellemare, Alex Graves, Martin Riedmiller, Andreas K Fidjeland, Georg Ostrovski, et al. Human-level control through deep reinforcement learning. *nature*, 518(7540):529–533, 2015.
- [43] Tung D Nguyen, Rui Shu, Tuan Pham, Hung Bui, and Stefano Ermon. Temporal predictive coding for model-based planning in latent space. In *International Conference on Machine Learning*, pages 8130–8139. PMLR, 2021.
- [44] Masashi Okada and Tadahiro Taniguchi. Dreaming: Model-based reinforcement learning by latent imagination without reconstruction. In *2021 IEEE International Conference on Robotics and Automation (ICRA)*, pages 4209–4215. IEEE, 2021.
- [45] Masashi Okada and Tadahiro Taniguchi. Dreamingv2: Reinforcement learning with discrete world models without reconstruction. In *2022 IEEE/RSJ International Conference on Intelligent Robots and Systems (IROS)*, pages 985–991. IEEE, 2022.
- [46] Aaron van den Oord, Yazhe Li, and Oriol Vinyals. Representation learning with contrastive predictive coding. *arXiv preprint arXiv:1807.03748*, 2018.
- [47] Keiran Paster, Lev E McKinney, Sheila A McIlraith, and Jimmy Ba. Blast: Latent dynamics models from bootstrapping. In *Deep RL Workshop NeurIPS 2021*, 2021.
- [48] Adam Paszke, Sam Gross, Francisco Massa, Adam Lerer, James Bradbury, Gregory Chanan, Trevor Killeen, Zeming Lin, Natalia Gimelshein, Luca Antiga, et al. Pytorch: An imperative style, high-performance deep learning library. *Advances in neural information processing systems*, 32, 2019.
- [49] Julian Schrittwieser, Ioannis Antonoglou, Thomas Hubert, Karen Simonyan, Laurent Sifre, Simon Schmitt, Arthur Guez, Edward Lockhart, Demis Hassabis, Thore Graepel, et al. Mastering atari, go, chess and shogi by planning with a learned model. *Nature*, 588(7839):604–609, 2020.
- [50] John Schulman, Filip Wolski, Prafulla Dhariwal, Alec Radford, and Oleg Klimov. Proximal policy optimization algorithms. *arXiv preprint arXiv:1707.06347*, 2017.

- [51] David Silver, Aja Huang, Chris J Maddison, Arthur Guez, Laurent Sifre, George Van Den Driessche, Julian Schrittwieser, Ioannis Antonoglou, Veda Panneershelvam, Marc Lanctot, et al. Mastering the game of go with deep neural networks and tree search. *nature*, 529(7587):484–489, 2016.
- [52] David Silver, Hado Hasselt, Matteo Hessel, Tom Schaul, Arthur Guez, Tim Harley, Gabriel Dulac-Arnold, David Reichert, Neil Rabinowitz, Andre Barreto, et al. The predictron: End-to-end learning and planning. In *International Conference on Machine Learning*, pages 3191–3199. PMLR, 2017.
- [53] David Silver, Thomas Hubert, Julian Schrittwieser, Ioannis Antonoglou, Matthew Lai, Arthur Guez, Marc Lanctot, Laurent Sifre, Dharshan Kumaran, Thore Graepel, et al. A general reinforcement learning algorithm that masters chess, shogi, and go through self-play. *Science*, 362(6419):1140–1144, 2018.
- [54] Richard S Sutton. Learning to predict by the methods of temporal differences. *Machine learning*, 3:9–44, 1988.
- [55] Richard S Sutton. Dyna, an integrated architecture for learning, planning, and reacting. *ACM Sigart Bulletin*, 2(4):160–163, 1991.
- [56] Yuval Tassa, Yotam Doron, Alistair Muldal, Tom Erez, Yazhe Li, Diego de Las Casas, David Budden, Abbas Abdolmaleki, Josh Merel, Andrew Lefrancq, et al. Deepmind control suite. *arXiv preprint arXiv:1801.00690*, 2018.
- [57] Aaron Van Den Oord, Oriol Vinyals, et al. Neural discrete representation learning. *Advances in neural information processing systems*, 30, 2017.
- [58] Oriol Vinyals, Igor Babuschkin, Wojciech M Czarnecki, Michaël Mathieu, Andrew Dudzik, Junyoung Chung, David H Choi, Richard Powell, Timo Ewalds, Petko Georgiev, et al. Grandmaster level in starcraft ii using multi-agent reinforcement learning. *Nature*, 575(7782):350–354, 2019.
- [59] Tingwu Wang and Jimmy Ba. Exploring model-based planning with policy networks. *arXiv preprint arXiv:1906.08649*, 2019.
- [60] Tingwu Wang, Xuchan Bao, Ignasi Clavera, Jerrick Hoang, Yeming Wen, Eric Langlois, Shunshi Zhang, Guodong Zhang, Pieter Abbeel, and Jimmy Ba. Benchmarking model-based reinforcement learning. *arXiv preprint arXiv:1907.02057*, 2019.
- [61] Manuel Watter, Jost Springenberg, Joschka Boedecker, and Martin Riedmiller. Embed to control: A locally linear latent dynamics model for control from raw images. *Advances in neural information processing systems*, 28, 2015.
- [62] Chen Wei, Haoqi Fan, Saining Xie, Chao-Yuan Wu, Alan Yuille, and Christoph Feichtenhofer. Masked feature prediction for self-supervised visual pre-training. In *Proceedings of the IEEE/CVF Conference on Computer Vision and Pattern Recognition*, pages 14668–14678, 2022.
- [63] Ronald J Williams. Simple statistical gradient-following algorithms for connectionist reinforcement learning. *Machine learning*, 8:229–256, 1992.
- [64] Zhenda Xie, Zheng Zhang, Yue Cao, Yutong Lin, Jianmin Bao, Zhuliang Yao, Qi Dai, and Han Hu. Simmim: A simple framework for masked image modeling. In *Proceedings of the IEEE/CVF Conference on Computer Vision and Pattern Recognition*, pages 9653–9663, 2022.
- [65] Denis Yarats, Rob Fergus, Alessandro Lazaric, and Lerrel Pinto. Mastering visual continuous control: Improved data-augmented reinforcement learning. *arXiv preprint arXiv:2107.09645*, 2021.
- [66] Weirui Ye, Shaohuai Liu, Thanard Kurutach, Pieter Abbeel, and Yang Gao. Mastering atari games with limited data. *Advances in Neural Information Processing Systems*, 34:25476–25488, 2021.
- [67] Jure Zbontar, Li Jing, Ishan Misra, Yann LeCun, and Stéphane Deny. Barlow twins: Self-supervised learning via redundancy reduction. In *International Conference on Machine Learning*, pages 12310–12320. PMLR, 2021.

A Appendix

A.1 Atari100k Benchmark

The Atari100k benchmark was proposed in Kaiser et al. [33] to evaluate reinforcement learning agents on Atari games in low data regime. The benchmark includes 26 Atari games with discrete actions and a budget of 400K environment steps, amounting to 100K policy steps using the default action repeat setting. This represents 2 hours of real-time play. The current state-of-the-art is held by EfficientZero (EffZero) [66], which uses look-ahead search to select the best action, with a human mean score of 190% and median of 116%. In this work, we compare our method with DreamerV3 and other model-based approaches which do not use look-ahead search.

Table 4: Atari100k scores (400K environment steps). We average the evaluation score over 10 episodes and use 5 different seeds per experiment.

Game	Random	Human	Lookahead search		No lookahead search			
			MuZero	EffZero	SimPLe	IRIS	DreamerV3	MuDreamer
Alien	228	7128	530	1140	617	420	959	951
Amidar	6	1720	39	102	74	143	139	153
Assault	222	742	500	1407	527	1524	706	891
Asterix	210	8503	1734	16844	1128	854	932	1411
Bank Heist	14	753	193	362	34	53	649	156
Battle Zone	2360	37188	7688	17938	4031	13074	12250	12080
Boxing	0	12	15	44	8	70	78	96
Breakout	2	30	48	406	16	84	31	34
Chopper Com.	811	7388	1350	1794	979	1565	420	808
Crazy Climber	10780	35829	56937	80125	62584	59324	97190	96128
Demon Attack	152	1971	3527	13298	208	2034	303	553
Freeway	0	30	22	22	17	31	0	5
Frostbite	65	4335	255	314	237	259	909	1652
Gopher	258	2412	1256	3518	597	2236	3730	1500
Hero	1027	30826	3095	8530	2657	7037	11161	8272
James Bond	29	303	88	459	100	463	445	409
Kangaroo	52	3035	63	962	51	838	4098	4380
Krull	1598	2666	4891	6047	2205	6616	7782	9644
Kung Fu Mas.	258	22736	18813	31112	14862	21760	21420	26832
Ms Pacman	307	6952	1266	1387	1480	999	1327	2311
Pong	-21	15	-7	21	13	15	15	18
Private Eye	25	69571	56	100	35	100	882	1042
Qbert	164	13455	3952	15458	1289	746	3405	4061
Road Runner	12	7845	2500	18512	5641	9615	15565	8460
Seaquest	68	42055	208	1020	683	661	618	428
Up N Down	533	11693	2897	16096	3350	3546	7600	26494
#Superhuman	0	N/A	5	13	1	10	9	11
Human Mean	0%	100%	56%	190%	33%	105%	112%	126%
Human Median	0%	100%	23%	116%	13%	29%	49%	43%

Table 4 compares MuDreamer with DreamerV3 [25] and other model-based approaches [49, 11, 36, 66, 40] on the Atari100k benchmark. Following preceding works, we compare the mean and median returns across all 26 games using human-normalized scores calculated as follow:

$$\text{norm_score} = (\text{agent_score} - \text{random_score}) / (\text{human_score} - \text{random_score}) \quad (10)$$

MuDreamer achieves results comparable to DreamerV3, without using a decoder reconstruction loss during training. Our implementation takes 4 hours and 40 minutes to reach 400K steps on the *Breakout* Atari game using a single NVIDIA RTX 3090 GPU and 16 CPU cores, while DreamerV3 takes 5 hours and 20 minutes.

A.2 Limitations

Certain limitations of our work arise from the fact that trajectories sampled from the replay buffer are off-policy, which requires the value predictor to fit the value of older policies that are no longer accurate. The resulting value function differs from the one learned by the critic network which fits the value of the current neural network policy thought the world model. While we found this to have no effect on performance, experimenting with off-policy correction [66], this may be the case when scaling up to larger model sizes and more complex tasks.

A.3 Ethics Statement

The development of autonomous agents for real-world applications introduces various safety and environmental concerns. In real-world scenarios, an agent might cause harm to individuals and damage to its surroundings during both training and deployment. Although using world models during training can mitigate these risks by allowing policies to be learned through simulation, some risks may still persist. This statement aims to inform users of these potential risks and emphasize the importance of AI safety in the application of autonomous agents to real-world scenarios.

A.4 MuDreamer Hyper-Parameters

Table 5: MuDreamer hyper-parameters applied to the DeepMind Visual Control Suite (DMC) and Atari100k benchmark. We apply the same hyper-parameters to all tasks except for the number of environment instances and the training ratio (number of replayed steps per policy step). Discount and Return Lambda values are kept the same for World Model and Actor Critic learning.

Parameter	Symbol	Setting
General		
Replay Buffer Capacity (FIFO)	—	10^6
Batch Size	B	16
Batch Length	T	64
Optimizer	—	Adam
Activation	—	LayerNorm + SiLU
Model Size	—	DreamerV3 Small
Input Image Resolution	—	64×64 RGB
Replayed Steps per Policy Step	—	512 (DMC) / 1024 (Atari100k)
Environment Instances	—	4 (DMC) / 1 (Atari100k)
World Model		
Number of Latents	—	32
Classes per Latent	—	32
Prediction Loss Scale	β_{pred}	1.0
Dynamics Loss Scale	β_{dyn}	0.95
Representation Loss Scale	β_{rep}	0.05
Learning Rate	α	10^{-4}
Adam Betas	β_1, β_2	0.9, 0.999
Adam Epsilon	ϵ	10^{-8}
Gradient Clipping	—	1000
Slow Value Momentum	τ	0.99
Model Discount	γ	0.997
Model Return Lambda	λ	0.95
Activation Representation Network	—	BatchNorm + SiLU
BatchNorm Momentum	—	0.9
Actor Critic		
Imagination Horizon	H	15
Discount	γ	0.997
Return Lambda	λ	0.95
Critic EMA Decay	—	0.98
Critic EMA regularizer	—	1.0
Return Normalization Percentiles	—	5^{th} and 95^{th}
Return Normalization Decay	—	0.99
Actor Entropy Scale	η	$3 \cdot 10^{-4}$
Learning Rate	α	$3 \cdot 10^{-5}$
Adam Betas	β_1, β_2	0.9, 0.999
Adam Epsilon	ϵ	10^{-5}
Gradient Clipping	—	100

A.5 Network Architecture Details

Table 6: Encoder network architecture. LN refers to Layer Normalization [2]. The encoder downsamples images with strided convolutions of kernel size = 4, stride = 2 and zero padding = 1.

Module	Output shape
Input image (o_t)	$3 \times 64 \times 64$
Conv2d + LN + SiLU	$32 \times 32 \times 32$
Conv2d + LN + SiLU	$64 \times 16 \times 16$
Conv2d + LN + SiLU	$128 \times 8 \times 8$
Conv2d + LN + SiLU	$256 \times 4 \times 4$
Flatten and Output features (x_t)	4096

Table 7: The Sequential Network process previous stochastic state z_{t-1} and action a_{t-1} to compute the next model hidden state h_t using a Gated Recurrent Unit (GRU) [13]. The GRU conditions the model hidden state on past context h_{t-1} which helps the world model to make accurate predictions. The initial GRU hidden state vector h_0 is learned via gradient descent among other network parameters and processed by the dynamics predictor to generate the initial stochastic state z_0 .

Module	Output shape
Input stochastic state (z_{t-1}), Input action (a_{t-1})	$32 \times 32, A$
Flatten and Concatenate	$1024 + A$
Linear + LN + SiLU	512
GRU and Output hidden state (h_t)	512

Table 8: The Representation Network process encoded features x_t and hidden state h_t to generate the model stochastic state z_t which is sampled from a one hot categorical distribution. We use batch normalization (BN) [32] inside the representation network to ensure stable training.

Module	Output shape
Input features (x_t), Input hidden state (h_t)	4096, 512
Concatenate	4608
Linear + BN + SiLU	512
Linear and Reshape	32×32
Sample one hot and Output stochastic state (z_t)	32×32

Table 9: The Dynamics Predictor learns to predict current stochastic state z_t without being conditioned on encoded features x_t . The sequential network and dynamics predictor are used during the behavior learning phase to generate imaginary trajectories and train the actor-critic networks.

Module	Output shape
Input hidden state (h_t)	512
Linear + LN + SiLU	512
Linear and Reshape	32×32
Sample one hot and Output stochastic state (\hat{z}_t)	32×32

Table 10: Networks with Multi Layer Perceptron (MLP) structure. Inputs are first flattened and concatenated along the feature dimension. Each MLP layer is followed by a layer normalization and SiLU activation except for the last layer which outputs distribution logits.

Network	MLP layers	Inputs	Hidden dimension	Output dimension	Output Distribution
Reward predictor	3	s_t	512	255	Symlog discrete
Continue predictor	3	s_t	512	1	Bernoulli
Value predictor	3	s_t	512	255	Symlog discrete
Action predictor	3	x_t, s_{t-1}	512	A	Normal (continuous) / One hot (discrete)
Critic network	3	s_t	512	255	Symlog discrete
Action network	3	s_t	512	A	Normal (continuous) / One hot (discrete)

A.6 World Model Predictions

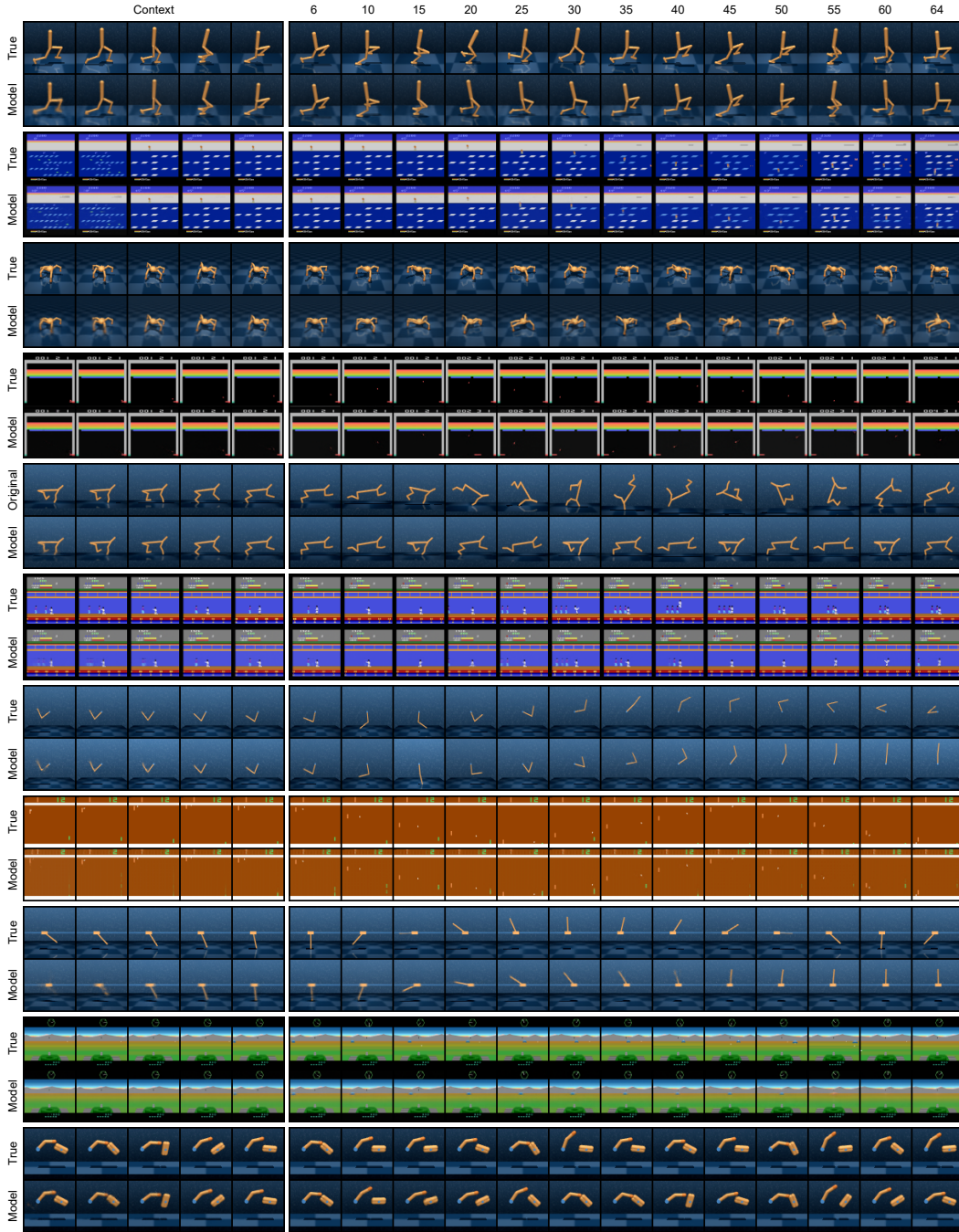


Figure 5: Trajectories imagined by the world model over 64 time steps using 5 context frames. MuDreamer generates accurate long-term predictions for various tasks without requiring reconstruction loss gradients during training to compress the observation information into the model hidden state. Although the reconstruction gradients are not propagated to the whole network, the decoder successfully reconstruct the input image, meaning that the model hidden state contains all necessary information about the environment.

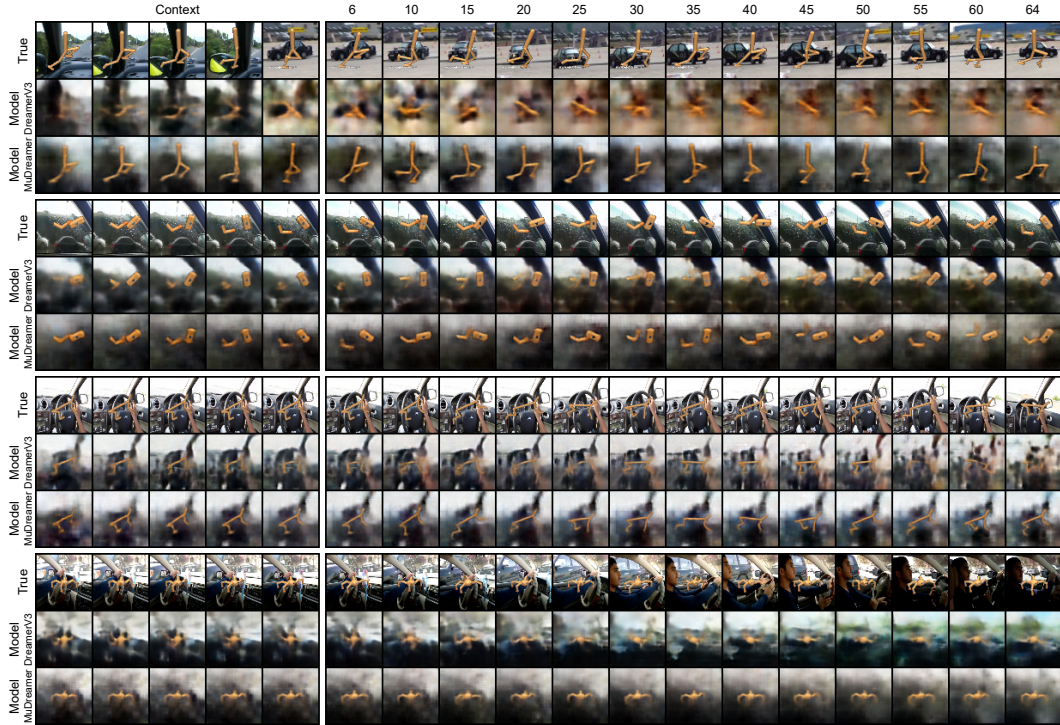


Figure 6: Trajectories imagined by DreamerV3 and MuDreamer world models over 64 time steps using 5 context frames under the natural background setting. MuDreamer models the environment dynamics in latent space, filtering the unnecessary information while DreamerV3 focuses on modeling the environment background.

A.7 Training Speed Comparison

We compare MuDreamer training speed and performance with Dreamer, TPC and DreamerPro. While MuDreamer achieves similar speed at test time, the training time and memory requirement are lowered due to the non-necessity of reconstructing input observations to learn hidden representations. Table 11 compares the training speed on the *Walker-run* visual control task using a RTX 3090 GPU. We show the number of FLOPs required for a world model training forward using a sequence of 64 time frames and same architecture hyper-parameters as MuDreamer (Table 5). We also experiment with larger image sizes, adding one strided convolution layer to the encoder and decoder networks when the image size is doubled. DreamerPro achieves competitive performance compared to MuDreamer but relies on the encoding of two augmented views of the same image to compute the SwAV loss. This results in a significant increase of the number of FLOPs and GPU memory, leading to slower training and memory overflow for larger image sizes. TPC benefits from good training speed since it does not require a decoder or action-value predictors but it also has a noticeable negative impact on performance.

Table 11: Training speed comparison on *Walker Run* task.

Method	Reconstruction Free Model	Single View Training	#FLOPs (Billion)			Training step per sec			Background Setting mean score
			64x64	128x128	256x256	64x64	128x128	256x256	
Dreamer [25]	✗	✓	4.3	7.0	18.0	4.6	2.8	OOM	86.7
TPC [43]	✓	✓	2.2	3.6	9.1	5.3	3.8	1.8	372.8
DreamerPro [15]	✓	✗	7.9	12.9	34.9	3.2	2.0	OOM	445.2
MuDreamer	✓	✓	2.5	3.8	9.3	5.0	3.7	1.8	517.0

A.8 Visual Control Suite Comparison

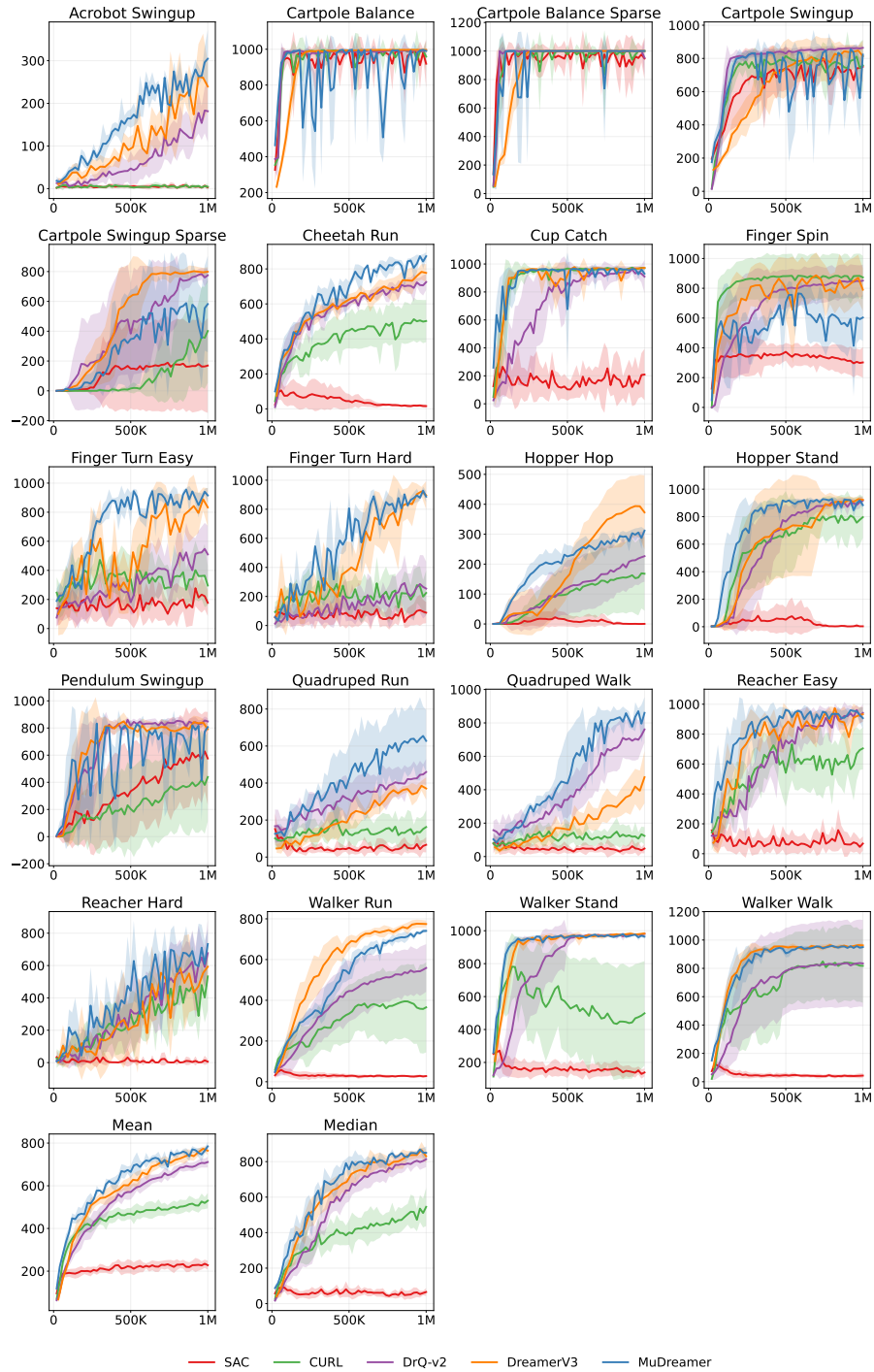


Figure 7: Comparison of MuDreamer with DreamerV3, DrQ-v2, CURL and SAC on the Deep Mind Control Suite (1M environment steps). We average the evaluation score over 10 episodes and use 3 seeds per experiment.

A.9 Natural Background Setting Comparison

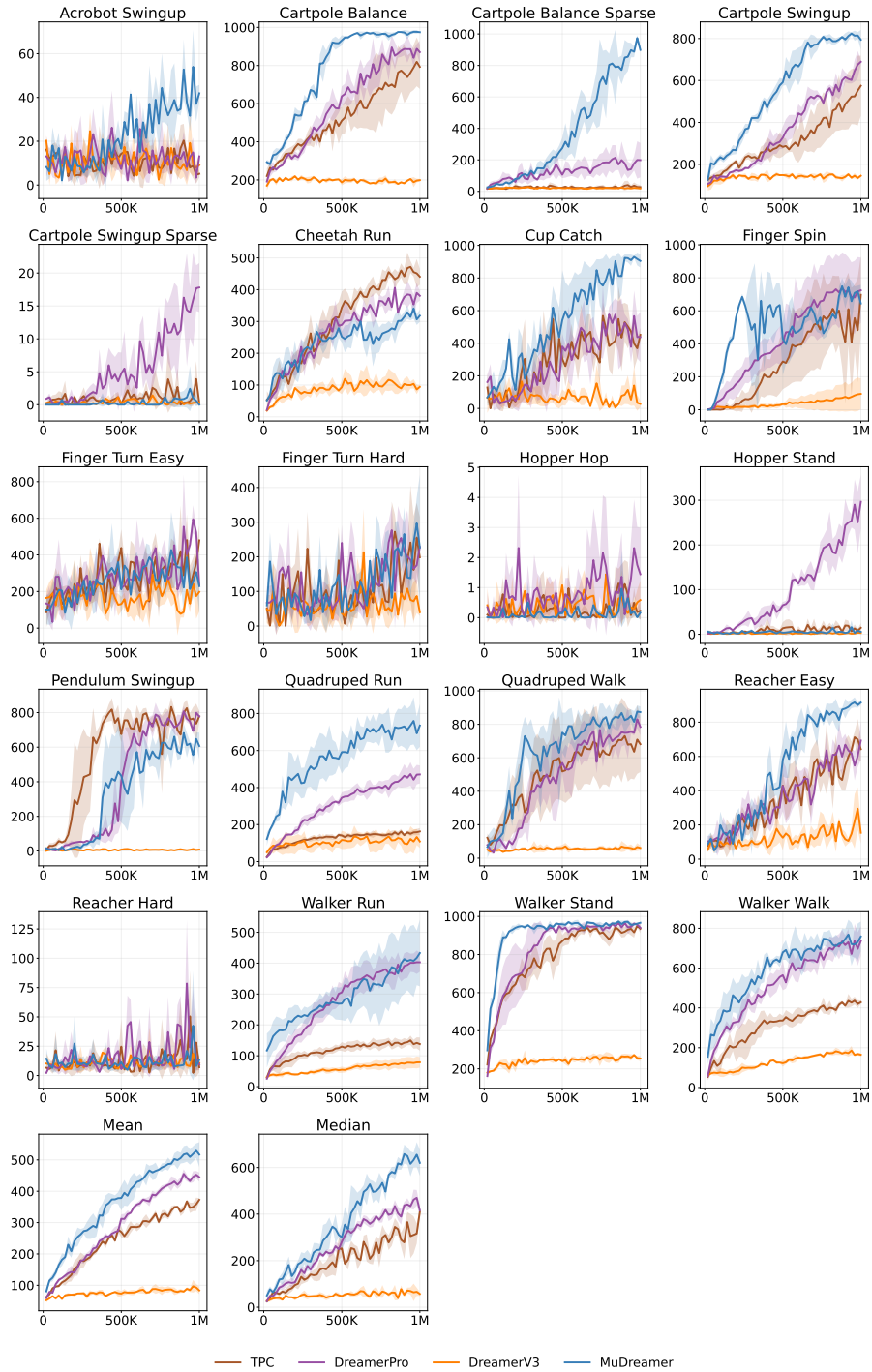


Figure 8: Comparison of MuDreamer with DreamerV3, DreamerPro and TPC under the natural background setting (1M environment steps). TPC and DreamerPro results were obtained using the official implementation of DreamerPro. We average the evaluation score over 10 episodes and use 3 seeds per experiment.

A.10 Atari100k Comparison

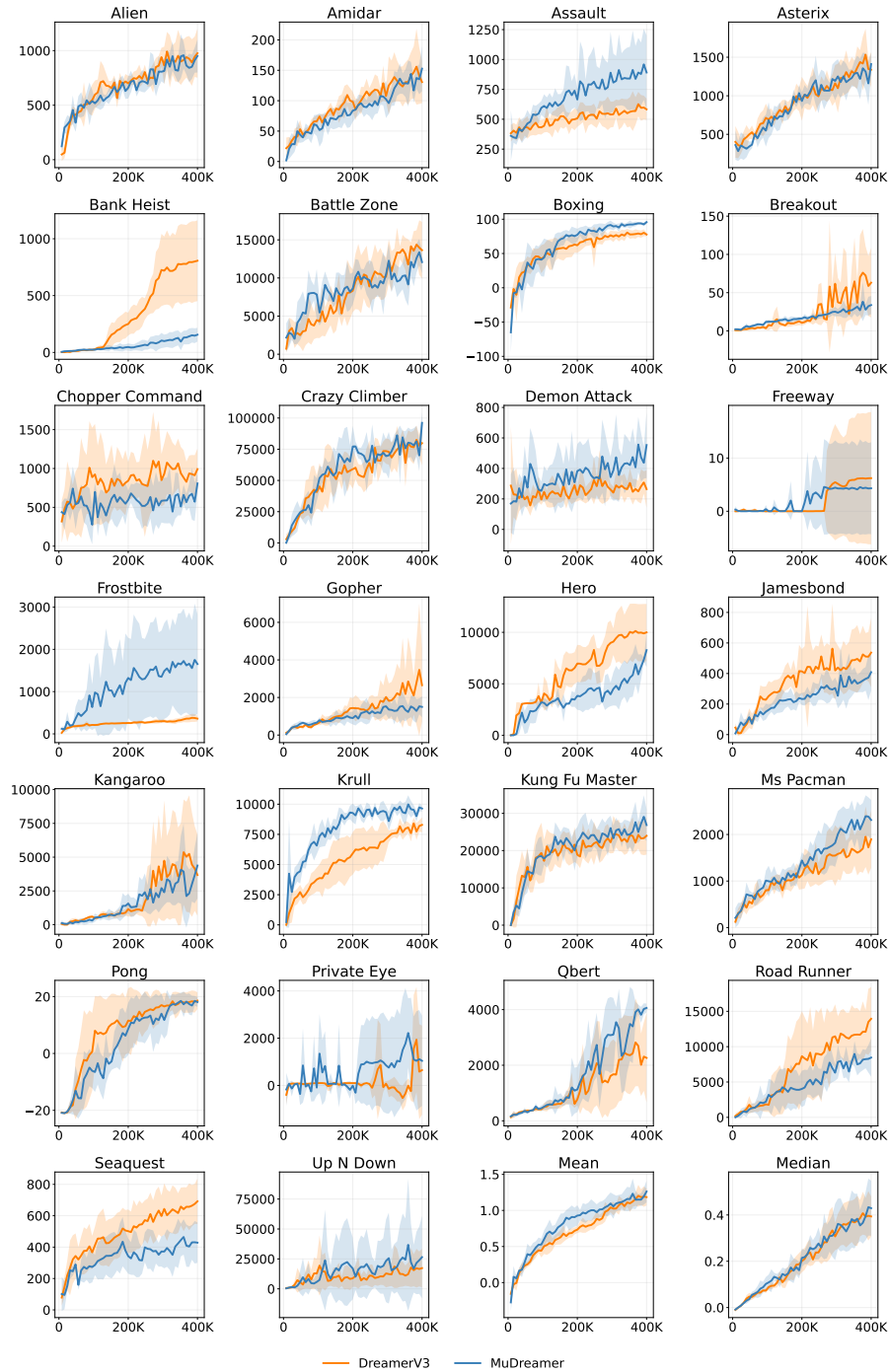


Figure 9: Comparison of MuDreamer and our tested re-implementation of the DreamerV3 algorithm on the Atari100k benchmark (400K environment steps). We average the evaluation score over 10 episodes and use 5 seeds per experiment.

A.11 Batch Normalization Ablation

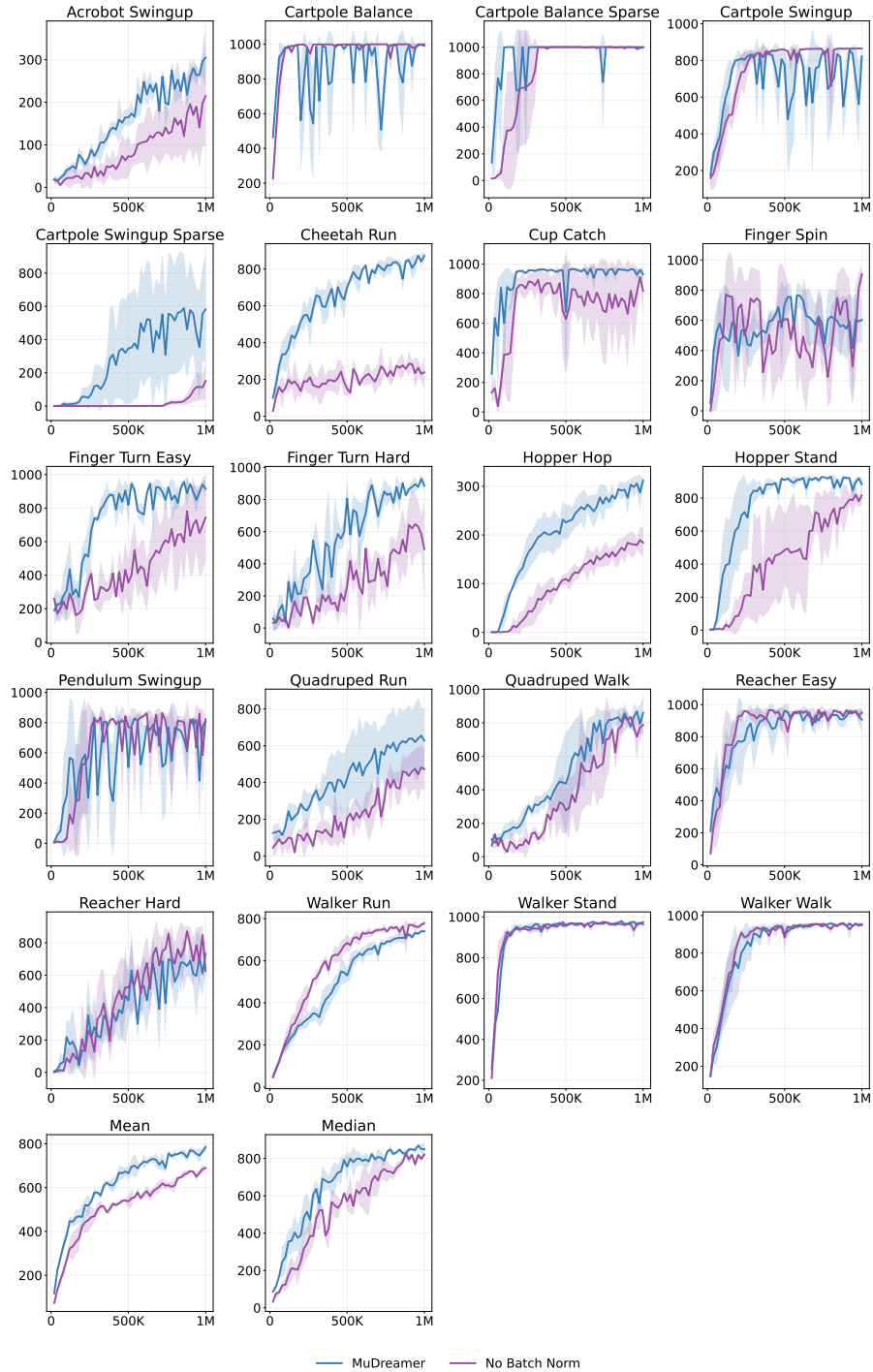


Figure 10: Comparison of MuDreamer, using layer normalization instead of batch normalization in the representation network. Removing the batch normalization layer leads to optimization difficulties for some of the tasks. The model hidden states collapse to constant or non-informative representations. This makes it impossible for the decoder to reconstruct the input observations.

A.12 Action and Value Predictors Ablation

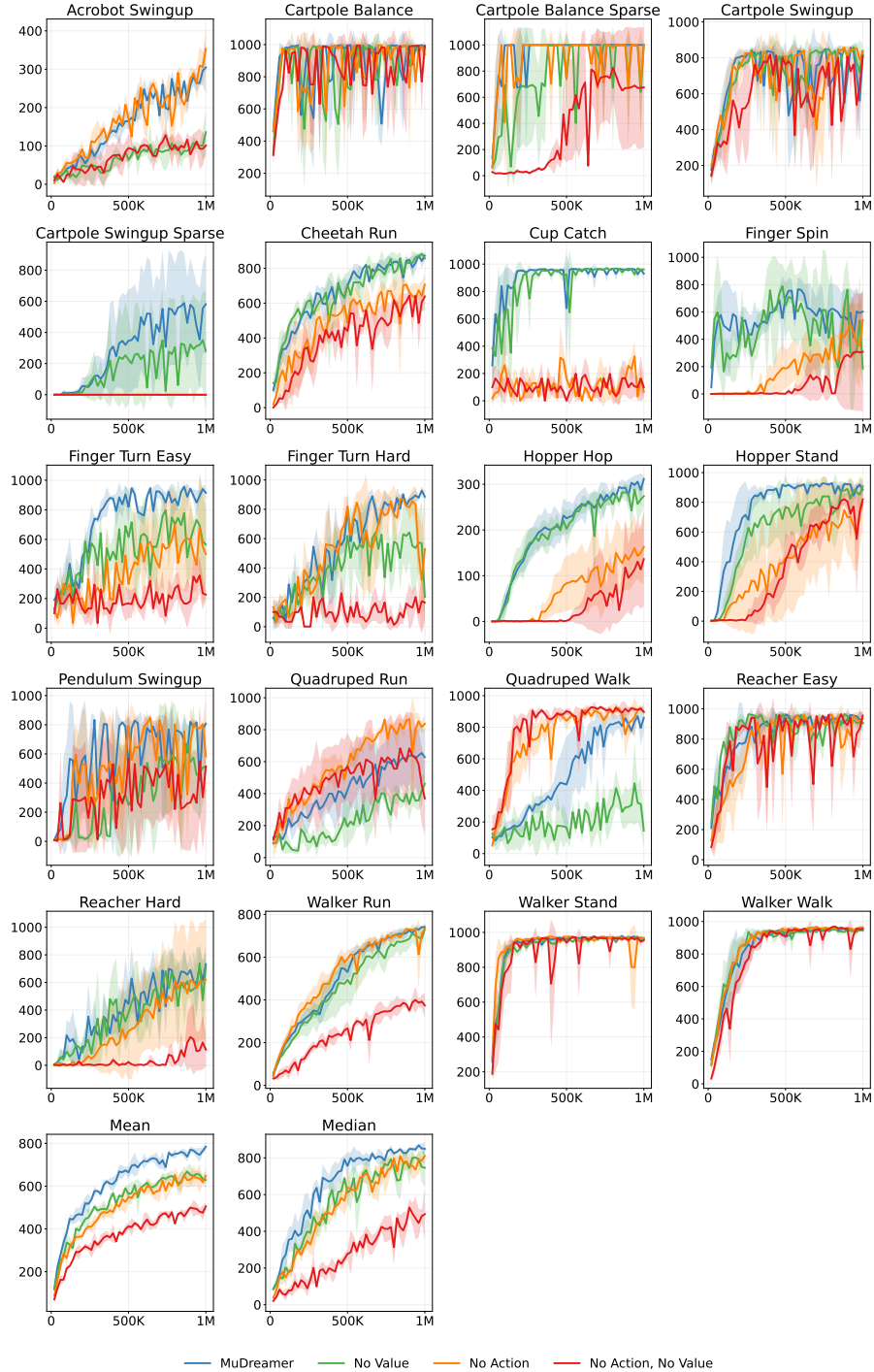


Figure 11: Comparison of MuDreamer, removing the action and/or value prediction heads. Removing the action and/or value heads during training deteriorates MuDreamer performance. We find that action prediction significantly helps tasks with sparse rewards like Hopper Hop or Cartpole Swingup Sparse. The value prediction head improves stability, leading to more stable learning. Both heads help the model to learn representations, leading to faster convergence and lower reconstruction loss.

A.13 KL Balancing Ablation

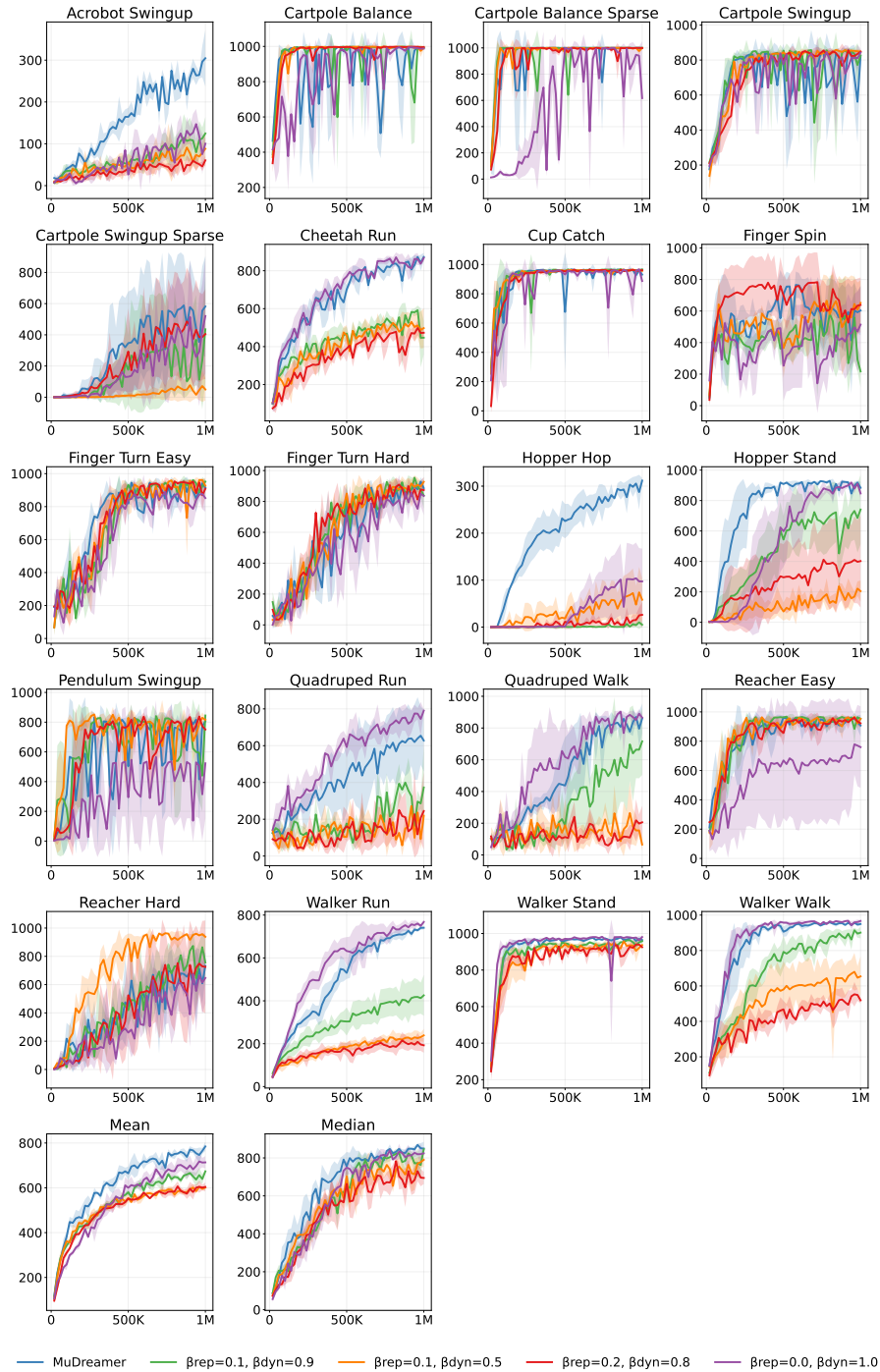


Figure 12: Comparison of MuDreamer, studying the effect of β_{dyn} and β_{rep} . We find that applying the default KL balancing parameters of DreamerV3 slows down convergence for some of the tasks, restraining the world model from learning representations. Setting β_{rep} to zero improves learning speed but results in instabilities and a degradation of performance after a certain amount of steps when training longer. Using a slight regularization of the representations toward the prior with $\beta_{rep} = 0.05$ improved convergence speed while maintaining stability.

A.14 Additional Visualizations

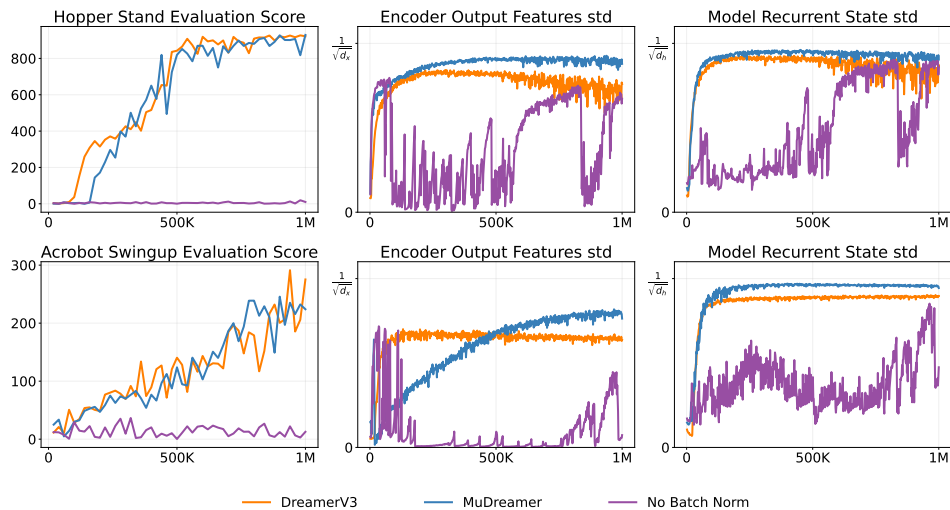


Figure 13: DreamerV3 and MuDreamer comparison with or without using batch normalization in the representation network instead of layer normalization (train ratio = 128). Left plots: agent evaluation score. Middle: the per-channel std of the l2-normalized encoder outputs x_t , plotted as the averaged std over all channels. Right plots: per-channel std of the l2-normalized model recurrent state h_t . Batch normalization improves learning stability and prevents collapses to constant feature vectors for all images.



Figure 14: Example of MuDreamer reconstruction on Walker Run and Cheetah Run tasks using default KL balancing parameters of DreamerV3 ($\beta_{dyn} = 0.5, \beta_{rep} = 0.1$). The default regularization of the posterior representations toward the prior tends to limit the amount of information in the latent space in order to minimize the KL divergence between the two state distributions. In this examples, we observe that unnecessary information such as the environment floor are reconstructed as monochrome surfaces without the original details.

A.15 Natural Background Setting 6 tasks Comparison

We compare MuDreamer with DreamerPro and TPC on the six visual control tasks considered in Deng et al. [15]. Following DreamerPro, we scale the reward prediction loss by a factor of 100 to further encourage extraction of task-relevant information. Figure 15 shows that MuDreamer outperforms DreamerPro and TPC over the six tasks without requiring encoding separate augmented views of input images during training. MuDreamer achieves a mean score of 661.3 over the six tasks against 562.4 and 453.3 for DreamerPro and TPC.

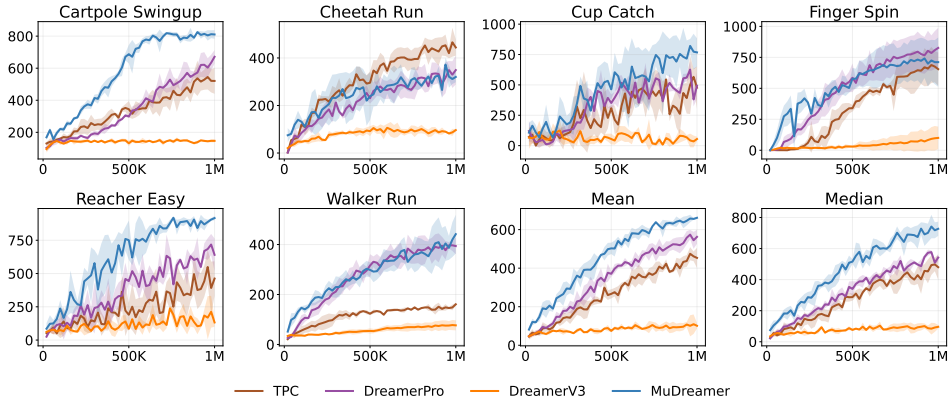


Figure 15: Comparison of MuDreamer with DreamerV3, DreamerPro and TPC on the six visual control tasks considered in Deng et al. [15] under the natural background setting (1M env. steps).

Table 12: Visual Control Suite scores on the six tasks considered in Deng et al. [15] under the natural background setting (1M environment steps). † denotes our tested reimplement of DreamerV3. ‡ results were taken from DreamerPro. We average the evaluation score over 10 episodes and use 3 seeds per experiment.

Task	TPC‡	DreamerPro‡	DreamerV3†	MuDreamer
Cartpole Swingup	520.7	671.2	146.8	810.4
Cheetah Run	444.2	349.1	96.5	320.1
Cup Catch	477.2	493.4	54.6	767.6
Finger Spin	654.8	826.4	99.8	711.5
Reacher Easy	462.1	640.6	132.3	916.7
Walker Run	160.7	393.8	76.5	441.6
Mean	453.3	562.4	101.1	661.3
Median	480.1	542.1	96.3	727.2